ELSEVIER

Nuclear Instruments and Methods in Physics Research A 456 (2000) 40–45

NUCLEAR INSTRUMENTS & METHODS IN PHYSICS RESEARCH Section A

www.elsevier.nl/locate/nima

Response uniformity of a large size RPC

G. Aielli, P. Camarri, R. Cardarelli, A. Di Ciaccio, L. Di Stante, B. Liberti, A. Paoloni*, R. Santonico

Dipartimento Fisica, Università di Roma, "Tor Vergata", INFN Sez. di Roma II, Via della Ricerca Scientifica 1, 00133 Roma, Italy

Abstract

The response uniformity of a 90×290 cm^2 RPC prototype working in avalanche mode has been tested using cosmic rays. The high statistics needed for the test has also been used for accurate efficiency studies. The intrinsic detector inefficiency free, from spacers effects has been measured.

Keywords: RPC; ATLAS muon trigger system; Response uniformity; Spacer; Primary ionization

1. Introduction

The response uniformity is an essential requirement for large RPC [1,2] systems, such as those utilized as trigger detectors in LHC experiments or in cosmic ray physics. Indeed, disuniformity of the detector response inside a single chamber would limit the extension of the efficiency plateau. Moreover, inomogeneities among different chambers would result in a complicate high-voltage distribution and control system.

The study of the performances of a real size ATLAS RPC prototype [4], reported on this paper, has been performed using cosmic rays in the INFN laboratories of the university of Rome "Tor Vergata".

2. Experimental layout

The experimental layout used in the present experiment is described in Fig. 1, which shows the test chamber together with the four RPC stations used for tracking cosmic muons. The size of the chamber under test is 90×290 cm^2. The tracking stations 1–3 have comparable sizes, but only 16 strips per view are read-out, so that the sensitive area is 50×50 cm^2. The lowest tracking station is a single-gap RPC, 50×50 cm^2 wide, located under a 15 cm thick lead shielding. The test chamber is movable with respect to the monitor telescope for scanning the entire area.

All the chambers work in avalanche regime with a gas mixture composed of $C_2H_2F_4$, C_4H_{10} and SF_6 in the volume ratios 96.65/3.00/0.35. Results with 0.5% SF_6 are also reported.

The read-out strips of all RPCs are 2.9 cm wide and the pitch is 3.1 cm. The monitor chambers work at 9.6 kV; their signals are amplified by a factor of 10 and discriminated with a threshold of 15 mV.

A scheme of the test chamber read-out is shown in Fig. 2: the RPC signals are amplified with a two-stage amplifier (gain = 250, bandwidth = 160 MHz), made of commercial components, and discriminated with a threshold of 60 mV.

* Corresponding author. Tel.: 062025028; fax: 062023507.
E-mail address: paoloni@roma2.infn.it (A. Paoloni).

0168-9002/00/$ - see front matter
PII: S0168-9002(00)00959-1

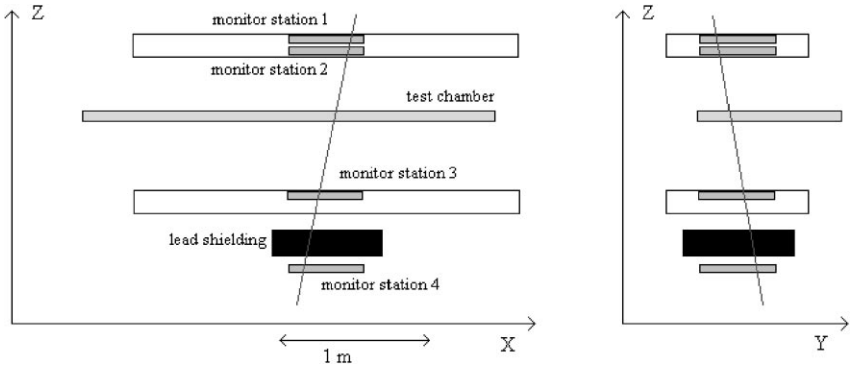

Fig. 1. Layout of the test.

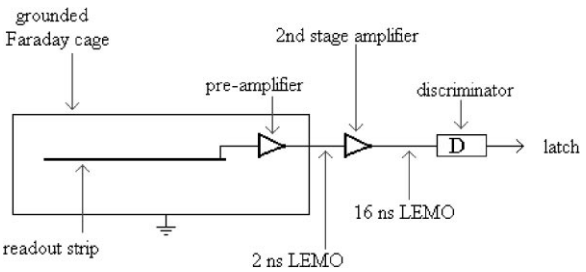

Fig. 2. Test chamber read-out scheme. The front-end electronics consists of a pre-amplifier with gain $\simeq 10$, which is located inside the chamber Faraday cage, and of a second stage amplifier with gain $\simeq 25$. Signals are discriminated with a threshold of 60 mV and coincidences with the trigger signal are registered with a latch.

The trigger signal, is the threefold coincidence between the ORed short strips of the layers 2–4. It is 60 ns shaped and is used to latch the signals from the monitor and from the test chamber, which are 100 ns shaped. Due to the lead shielding, the muons selected by the trigger system have energy above 200 MeV.

3. Description of the tracking algorithm

The tracks used in the analysis are selected according to the following criteria:

- only one cluster of size ≤ 3 strips in each layer of the monitor RPCs;
- straight trajectory reconstructed in both projections of the monitor chambers with $\chi^2/\text{dof} < 1.1$.

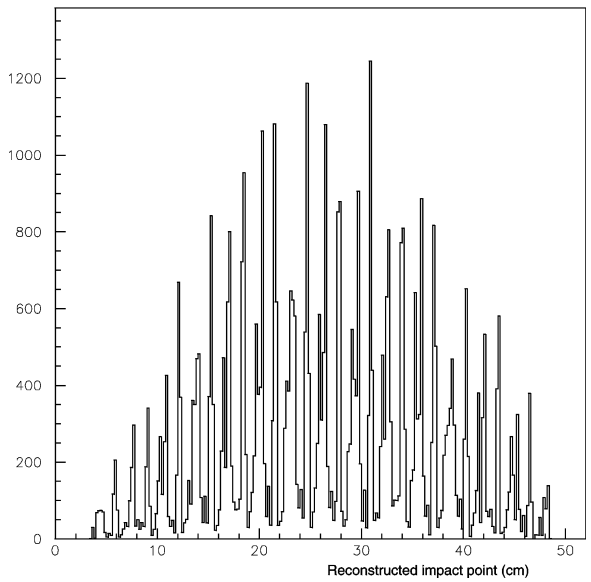

Fig. 3. X-projection of the reconstructed impact point on the test chamber. The spike structure is due to the discrete hits position on the monitor chambers.

The distribution of the reconstructed impact points on the test chamber is shown in Fig. 3. The spike structure in the distribution is due to the discrete position of the hits on the monitor chambers. The resolution of the tracking is better than 1 cm, as can be seen from the distribution of the residuals in Fig. 4 for events having cluster size ≤ 3 strips in the test chamber. The multipeak shaped distribution is due to the structure of the reconstructed impact points of

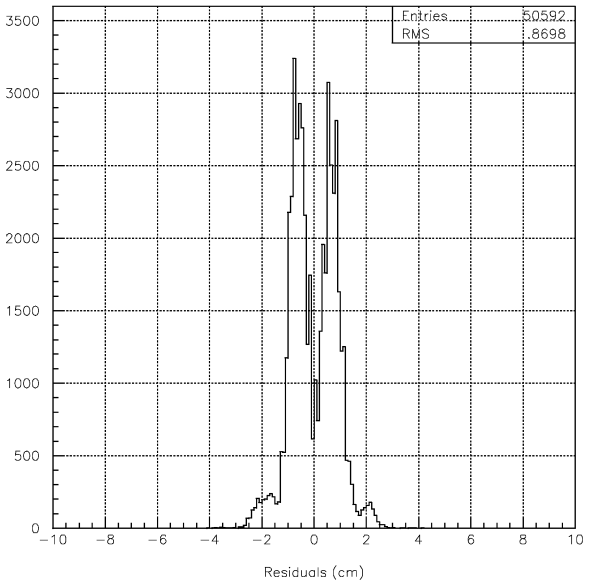

Fig. 4. Residuals distribution for X-projection. The considered sample is composed of events with cluster size ≤ 3 strips in the test chamber, which are 97% of the total number of the events selected at 9.7 kV.

Fig. 3 which combines with the discrete test chamber read-out.

4. Response uniformity test

A potential source of disuniformity is the gas gap thickness. To ensure its uniformity, the detector layout is characterized by a regular array of polycarbonate spacers [4] at a fixed distance of 10 cm from one another. The large-scale (> 10 cm) uniformity has been investigated by subdividing the test chamber into 12 pads of area 50×50 cm^2, covering the whole detector surface with some overlap. For each pad, the efficiency has been measured at different operating voltages; the tested RPC is considered efficient if there is a cluster matching the reconstructed track.

In order to take into account, the different environment conditions during data-taking, operating voltages have been normalized [3,5] according to the formula: $V = V_{\text{sper}} \times (T/T_0) \times P_0/P$, where

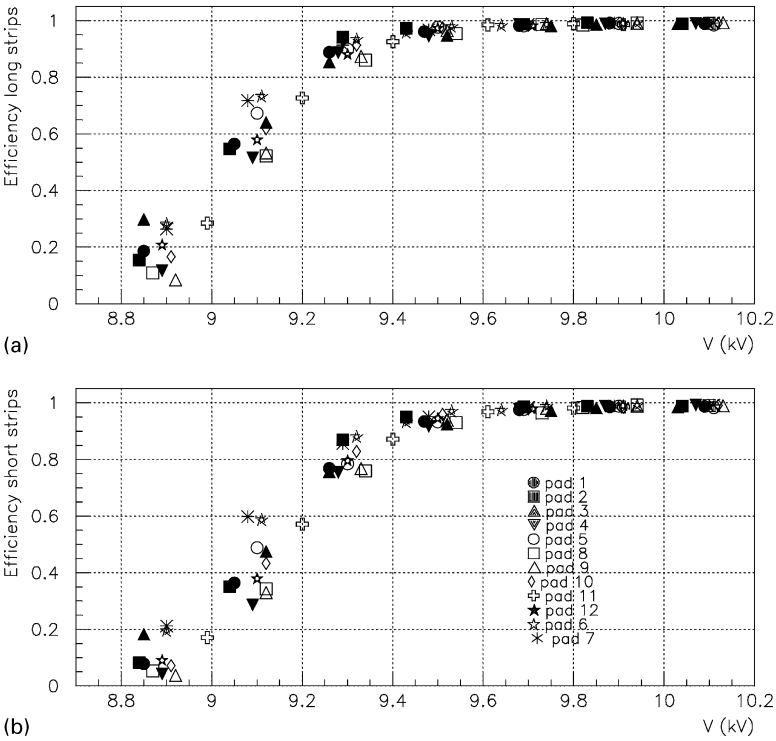

Fig. 5. Pads efficiency plots for longitudinal (a) and transversal (b) strips.

V_{sper}, P and T are the operating voltage, pressure and absolute temperature; V is the voltage normalized at $T_0 = 293$ K and $P_0 = 1010$ mbar.

In Fig. 5, the efficiency plots for transverse and longitudinal strips are shown. The operating voltages corresponding to 50% detection efficiency are contained within ± 60 V for all the pads. Interpreting this in terms of gap disuniformity, it corresponds to a variation of ± 13 μm on 2 mm, to be compared with the maximum spacer thickness tolerance, which is ± 15 μm.

5. Inefficiency analysis

A detailed analysis of the detector inefficiency has been made using a sample of about 53 000 muons collected all over the chamber-sensitive area at a normalized voltage of about 9.7 kV. In order to study the intrinsic detector efficiency, the OR of longitudinal and transverse strips is considered for efficiency calculations. The overall efficiency on the sample is $\varepsilon = (98.560 \pm 0.052)\%$.

With the purpose of studying the short-scale (≤ 10 cm) uniformity, we report in Fig. 6 the distribution of the inefficiency as a function of the distance, r, between the reconstructed track and the centre of the closest spacer.

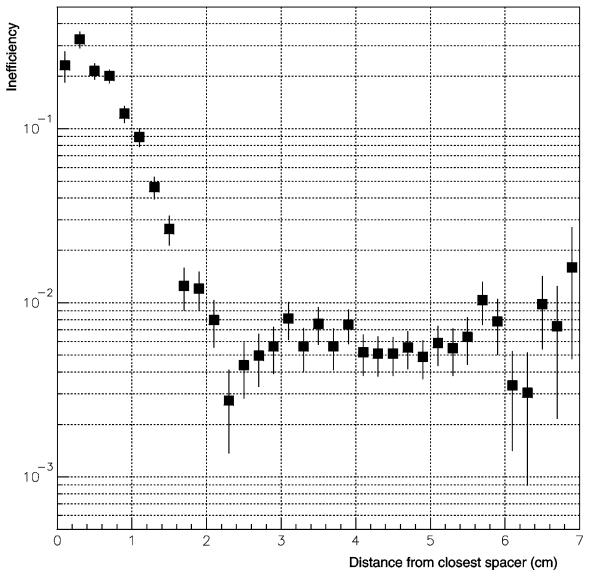

Fig. 6. RPC inefficiency distribution as a function of the distance between the reconstructed track and the centre of the closest spacer.

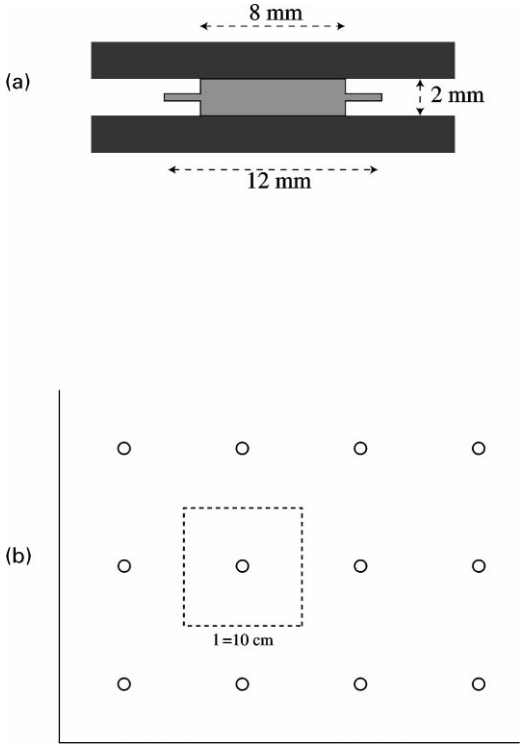

Fig. 7. Detailed sketch of a spacer (a) and elementary cells subdivision of an RPC (b). The spacer is composed of an inner cylinder of radius $r_i = 0.4$ cm and an outer "guard ring" of radius $r_o = 0.6$ cm.

The distribution exhibits a peak at $r = 0$ cm, due to the spacers, extending till to $r = r_{cut} = 2.2$ cm because of the coarse tracking resolution. For $r > r_{cut}$ the inefficiency is independent of r, and it is interpreted as the chamber intrinsic inefficiency $(1 - \varepsilon)_{int} = (0.584 \pm 0.036)\%$.

A detailed sketch of a spacer is shown in Fig. 7; the spacers contribution to the inefficiency can be schematized by describing them as an insensitive circle of radius r_{eff}. In such a scheme the efficiency for $r < r_{cut}$ is given by $\varepsilon_{cut} = (\pi r_{cut}^2 - \pi r_{eff}^2)/(\pi r_{cut}^2)\varepsilon_{int}$, which allows to evaluate r_{eff} as $r_{eff} = r_{cut} \times \sqrt{(\varepsilon_{int} - \varepsilon_{cut})/\varepsilon_{int}}$.

The plots of Fig. 8 show that r_{eff} is independent of the operating voltage. The values obtained from the large-statistics sample and from the fits

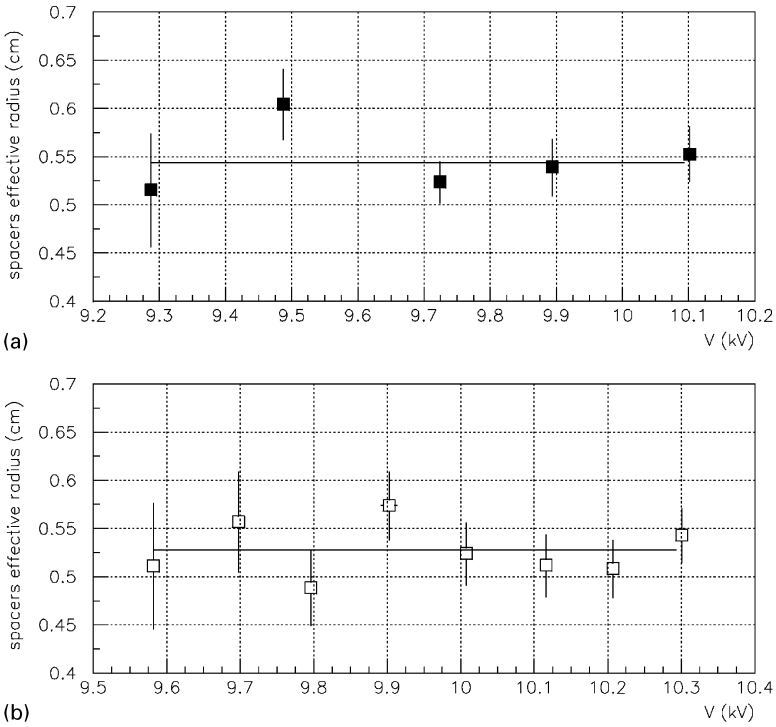

Fig. 8. Effective spacer radius as a function of the operating voltage for 0.35% SF_6 (a) and 0.5% SF_6 (b). The fit results are $r_{\rm eff} = (0.544 \pm 0.013)$ cm for (a) and $r_{\rm eff} = (0.527 \pm 0.013)$ cm for (b). Both values are consistent with the value estimated from the large statistics sample: $r_{\rm eff} = (0.522 \pm 0.013)$ cm.

of Fig. 8 are consistent with each other. Their average is $\langle r_{\rm eff} \rangle = (0.531 \pm 0.008)$ cm, which is to be compared with the actual spacer radius, $r_{\rm o} = 0.6$ cm.

As shown in Fig. 7, the spacers subdivide an RPC into elementary squared cells of side $l = 10$ cm, which is equal to the distance between two contiguous spacers. The spacer's contribution to the overall inefficiency can therefore be evaluated as $(1 - \varepsilon)_{\rm sp} = (\pi r_{\rm eff}^2)/l^2 = (0.886 \pm 0.027)\%$, which is larger than the intrinsic inefficiency.

The intrinsic inefficiency plots for the two considered gas mixtures exhibit a shift of about 200 V between them.

6. Intrinsic inefficiency and primary ionization

If we interpret the inefficiency as the "zero-probability" of a Poisson distribution, the intrinsic inefficiency can be parameterized as $(1 - \varepsilon)_{\rm int} = {\rm e}^{-n}$,

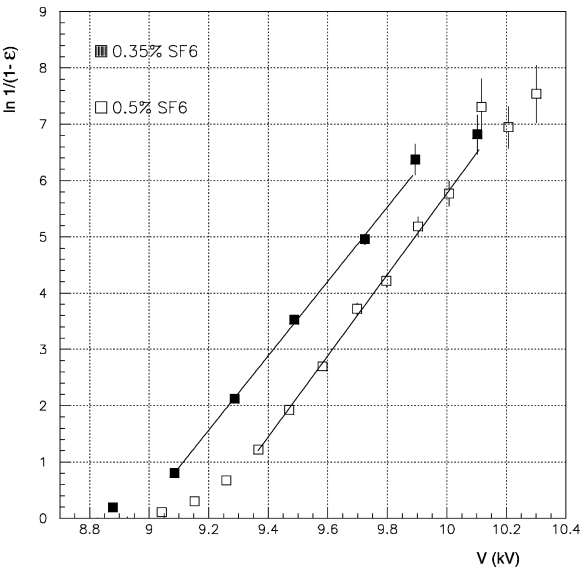

Fig. 9. Average number of effective primary ionizations vs. operating voltage for 0.35% and 0.5% SF_6. The total number of primary ionizations inside the gas gap, estimated from the Argon primary ionization normalized for the atomic number of tetrafluoroethane, is $n_{\rm tot} = 17$.

Table 1
$\Delta n/\Delta V$ and V_0 extrapolated at $n = 0$ for the two different SF_6 percentages

	$SF_6 = 0.35\%$	$SF_6 = 0.5\%$
B (ionizations/kV)	6.608 ± 0.021	7.204 ± 0.040
V_0 (kV)	8.963 ± 0.040	9.199 ± 0.073

where n is the average effective number of primary ionizations contributing to detector efficiency in the actual set-up.

The plots of $n = \ln 1/((1 - \varepsilon)_{\text{int}})$ are shown on Fig. 9. For efficiencies above 70% ($n > 1.2$) the data fit a straight line. In Table 1 the angular coefficient, B, and the voltage extrapolated at $n = 0$, V_0, are reported for the two gas mixtures.

7. Conclusions

The operating voltage of a large size RPC was found to be uniform within ± 60 V over the whole detector area.

Spacers are the principal source of inefficiency and their contribution to the overall inefficiency does not exceed the value expected from their size (1% of the total detector-sensitive area).

The intrinsic detector efficiency well inside the plateau region is better than 99.5%. The effective number of primary ionizations, which determines the intrinsic efficiency, increases linearly with the operating voltage up to a value of about 7.

References

[1] R. Santonico, R. Cardarelli, Nucl. Instr. and Meth. A 377 (1981) 187.
[2] R. Cardarelli et al., Nucl. Instr. and Meth. A 263 (1988) 200.
[3] M. Abbrescia et al., Nucl. Instr. and Meth. A 359 (1995) 603.
[4] The ATLAS Collaboration, ATLAS Muon Spectrometer Technical Design Report, CERN/LHCC 97-22 (1997) 281.
[5] P. Camarri et al., Nucl. Instr. and Meth. A 414 (1998) 317.